ELSEVIER

Biochemical Pharmacology 63 (2002) 1863–1873

Biochemical Pharmacology

Metal-organic compounds: a new approach for drug discovery *N*1-(4-methyl-2-pyridyl)-2,3,6-trimethoxybenzamide copper(II) complex as an inhibitor of human immunodeficiency virus 1 protease

Florence Lebon[a,1], Nicole Boggetto[b,1], Marie Ledecq[a], François Durant[a], Zohra Benatallah[c], Sames Sicsic[c], René Lapouyade[d,2], Olivier Kahn[d,†], Ange Mouithys-Mickalad[e], Ginette Deby-Dupont[e], Michèle Reboud-Ravaux[b,*]

[a]*Facultés Universitaires Notre-Dame de la Paix, Laboratoire de Chimie Moléculaire Structurale, 61 rue de Bruxelles, 5000 Namur, Belgium*
[b]*Laboratoire d'Enzymologie Moléculaire et Fonctionnelle, Département de Biologie Cellulaire, Institut Jacques Monod, CNRS-Universités Paris 6 and 7, 2 Place Jussieu, F-75251 Paris Cedex 05, France*
[c]*Laboratoire de Reconnaissance Moléculaire et Cellulaire, Biocis (UPRES-A CNRS 8076), Faculté de Pharmacie, 5 rue J.B. Clément, 92296 Châtenay-Malabry Cedex, France*
[d]*Laboratoire des Sciences Moléculaires, Institut de Chimie de La Matière Condensée de Bordeaux, Avenue du Dr. Schweitzer, 33608 Pessac Cedex, France*
[e]*Université de Liège, CORD-Centre de l'Oxygène Recherche et Développement B6A, Sart-Tilman, 4000 Liège, Belgium*

Received 28 September 2001; accepted 22 February 2002

Abstract

The use of metal-organic complexes is a potentially fruitful approach for the development of novel enzyme inhibitors. They hold the attractive promise of forming stronger attachments with the target by combining the co-ordination ability of metals with the unique stereoelectronic properties of the ligand. We demonstrated that this approach can be successfully used to inhibit the protease of the human immunodeficiency virus (type 1). Several ligands bearing substituents designed to interact with the catalytic site of the enzyme when complexed to Cu^{2+} were synthesised. The inhibition pattern of the resulting copper(II) complexes was analysed. We showed that the copper(II) complex of *N*1-(4-methyl-2-pyridyl)-2,3,6-trimethoxybenzamide (**C1**) interacts with the active site of the enzyme leading to competitive inhibition. On the other hand, *N*2-pyridine-amide ligands and oxazinane carboxamide ligand were found to be poor chelators of the cupric ion under the enzymatic assay conditions. In these cases, the observed inhibition was attributed to released cupric ions which react with cysteine residues on the surface of the protease. While unchelated metal cations are not likely to be useful agents, metal chelates such as **C1** should be considered as promising lead compounds for the development of targeted drugs.

Keywords: HIV-1 protease; Antiprotease; AIDS; Inhibition; Metal-organic complexes; Copper complexes

1. Introduction

Recently, western countries have recorded a decrease in the death rate imputed to acquired immunodeficiency syndrome (AIDS). This success has been largely attributed to chemotherapies that abolish the infectivity of the predominant causative agent, the HIV-1, by inhibiting essential viral enzymes. One of these is the PR whose activity is a prerequisite for viral replication. Two main sites have been identified as potential targets for the inhibition of HIV-1 PR, the active site [1–4] and the interface [5,6], the latter being largely responsible for the stabilisation of the enzyme dimeric structure. The compounds that have reached clinical application to date target the active site of HIV-1 PR [7,8]. These molecules act as transition state analogues and were designed by modifying the natural peptidic scaffold into peptidomimetics. However, mutations

* Corresponding author. Tel.: +33-1-44275078; fax: +33-1-44275994.
E-mail address: reboud@ccr.jussieu.fr (M. Reboud-Ravaux).

[1] These authors contributed equally to this work.

[2] Present address: Laboratoire d'Analyse Chimique par Reconnaissance Moléculaire(LACReM), Ecole Nationale Supérieure de Chimie et de Physique de Bordeaux (ENSCPB), Pessac, France.

[†] Deceased.

Abbreviations: HIV-1, human immunodeficiency virus type I; PR, protease; EPR, electron paramagnetic resonance; MEP, molecular electrostatic potentials.

0006-2952/02/$ – see front matter
PII: S0006-2952(02)00918-8

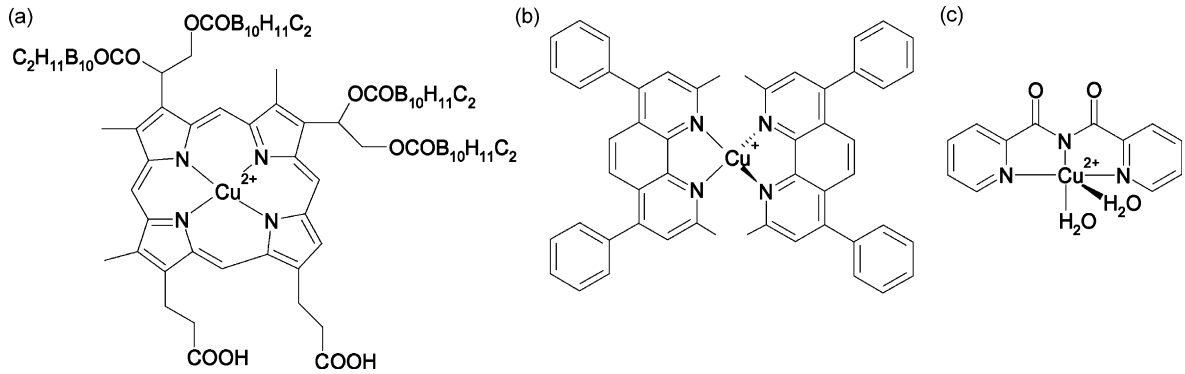

Fig. 1. Metal-organic inhibitors of HIV-1 PR reported in the literature: (a) porphyrin derivative ($IC_{50} = 0.975$ μM) [17], (b) BCDS-Cu(I) ($K_i = 1$ μM) [18], (c) setcez ($K_i = 480$ μM) [10].

in HIV-1 PR that bypass the action of the protease inhibitors appear rapidly and thus there is still an urgent need for novel families of inhibitors. We have used *de novo* drug design to investigate the potency of metal-organic compounds to act as inhibitors of the HIV-1 PR [9,10]. Enzyme inhibitors used as therapeutic agents are usually organic molecules that interact mainly with the proteins through hydrogen bonding and van der Waals contacts. Metal-organic complexes hold the attractive promise of forming stronger attachments with the target by combining the co-ordination ability of metals (covalent and ionic bonding) with the stereoelectronic properties of the ligand (hydrogen bonding and van der Waals contacts) [11,12]. Complexes with transition metals have previously been used to inhibit proteins [13–16]. Only a few such compounds have been reported as inhibitors of HIV-1 PR (Fig. 1). Metal-bound porphyrins which are non-peptide compounds with useful pharmacological properties, were identified as micromolar inhibitors of HIV-1 PR [17]. Bathocuproine sulfonic acid-Cu(I) [BCDS-Cu(I)] was found to be a competitive inhibitor of HIV-1 PR [18]. BCDS alone did not inhibit the enzyme and the inhibition could not be attributed to free Cu(I) ions: the inhibition by the complex remained in the presence of ethylenediaminetetraacetic acid (EDTA), which is known to prevent PR inhibition by uncomplexed metals. These two features indicated that the metal complex was the active inhibitor. However, these compounds did not emerge from a rational design aimed at using the unique structural properties of metal-organic complexes. We based our design on the hypothesis that a metal ion could bind HIV-1 PR structural catalytic water molecule and further block the activity of the enzyme. We used the distinct Cu^{2+} co-ordination geometry to design ligands that would further bind selectively HIV-1 PR binding pockets (Fig. 2). Based on this design, we reported that compound diaqua [bis(2-pyridylcarbonyl) amido] copper(II) nitrate dihydrate (setcez) behaves as a poor competitive inhibitor ($K_i = 480 \pm 120$ μM) of the PR [10]. Docking of this compound into the active site of HIV-1 PR shows that the side chains of the chelated ligand only partially occupy the enzyme subsites. Larger ligands that could fit into the HIV-1 PR binding site when complexed to Cu^{2+} were designed to improve the binding affinity of the metal-organic complex. Compounds *N*1-(4-methyl-2-pyridyl)-2,3,6-trimethoxybenzamide (**1**), *N*2-(2-methoxybenzyl)-2-quinolinecarboxamide (**2**), *N*2-(2-methoxybenzyl)-6-phenyl-1,3-oxazinane-2-carboxamide (**7**), *N*2-benzyl-2-quinolinecarboxamide (**8**), *N*2-(2-cyclohexyl)-2-quinolinecarboxamide (**9**) were synthesized and complexed to Cu^{2+} leading to complexes **C1**, **C2**, **C7**, **C8**, and **C9** respectively (Fig. 3). Complexes **C1**, **C2**, and **C9**, obtained by crystallography, adopt a tetragonally elongated octahedral geometry. Two ligands symmetrically co-ordinate copper(II) by aromatic nitrogen and amide oxygen atoms, forming an equatorial square plane [9]. The apical positions are occupied in the crystal by methanol or perchlorate molecules. No crystallographic data was obtained for complexes **C7** and **C8**. We describe herein the inhibition pattern analysis of this new family of metal-organic compounds targeting HIV-1 PR through kinetic experiments, EPR and molecular modelling techniques.

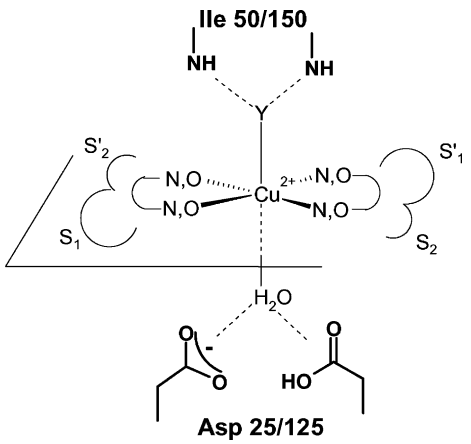

Fig. 2. Pharmacophore for the inhibition of HIV-1 PR by copper(II) co-ordination compounds. The enzyme residues are represented in bold style. Two ligands adopt an octahedral geometry able to organise the interaction elements into the shape of the active site of the PR. Y represents an H-bond acceptor. S1/S′1 and S2/S′2 represent the enzyme subsites following Schechter and Berger nomenclature [33].

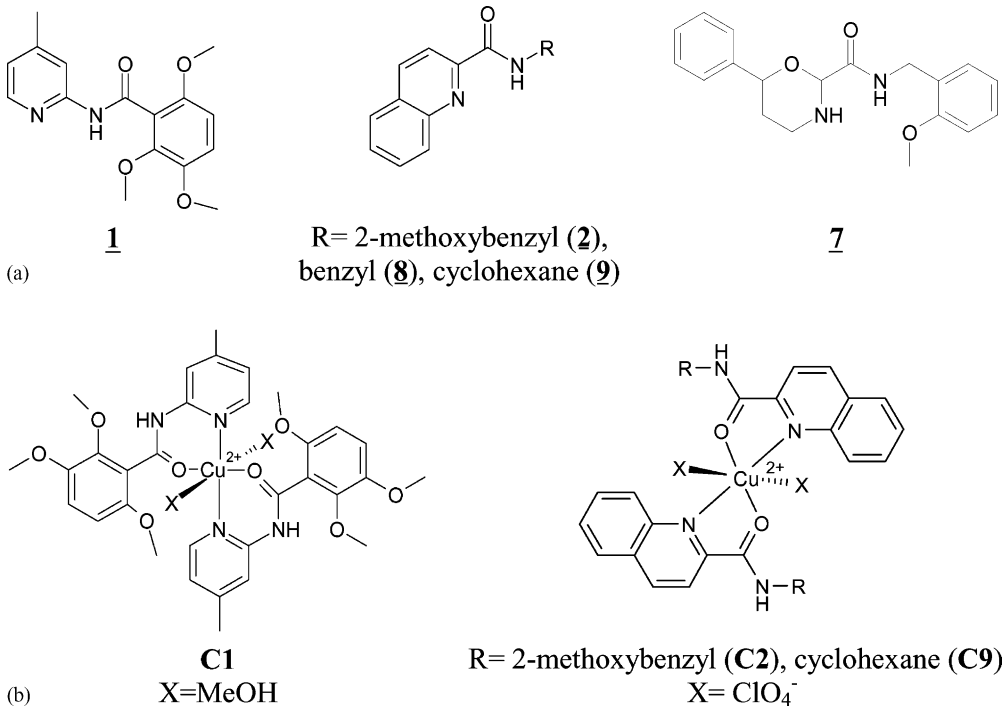

Fig. 3. (a) Structure of the pyridine-amide and oxazinane carboxamide ligands studied, (b) crystallographic structure of complexes **C1**, **C2**, and **C9**.

2. Experimental procedures

2.1. Synthesis

Caution! Perchlorate salts are potentially explosive. Although no detonation tendencies have been observed, caution is advised and handling of small quantities is recommended.

2.1.1. N1-(4-Methyl-2-pyridyl)-2,3,6-trimethoxybenzamide (*1*) and N2-(2-methoxybenzyl)-2-quinolinecarboxamide (*2*)

The synthesis of compounds **1** and **2** was previously reported [9].

The synthesis of compound **7** was achieved through classical methods, requiring the preparation of intermediate compounds **4**, **5**, and **6** (Scheme 1).

2.1.2. N1-(2-Methoxybenzyl)-2,2-di(isopropylsulfanyl)acetamide (*4*)

Following the method described by Qasmi *et al.* [19], to a solution of **3** (5 g, 24 mmol) in anhydrous CH_2Cl_2 (100 mL) was added successively at 0° under an argon atmosphere oxalyl chloride (6.28 mL, 72 eq) and dimethylformamide (0.8 mL). The reaction mixture was stirred at 0° for 1 hr and then concentrated *in vacuo*. The resulting concentrate was dissolved in CH_2Cl_2 (100 mL). To the mixture cooled at 0°, was added dropwise 2-methoxybenzylamine

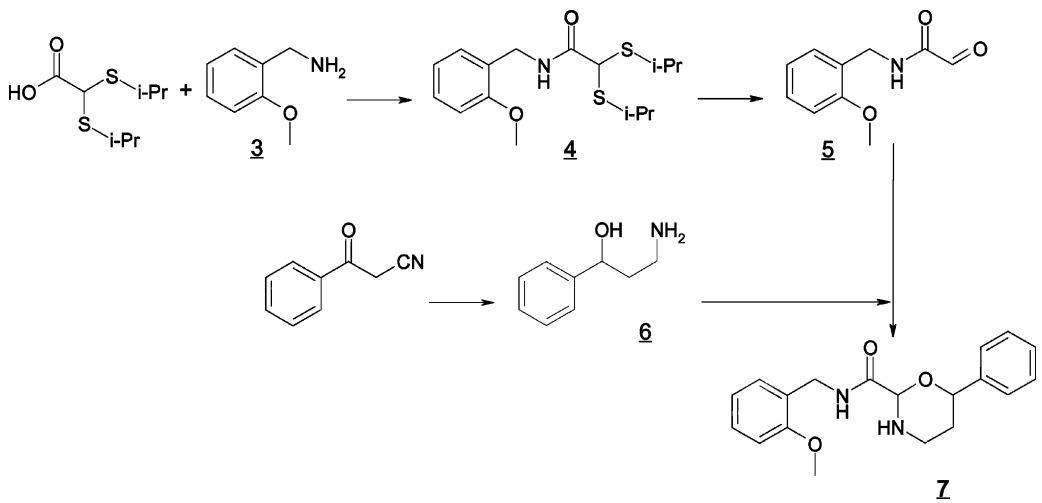

Scheme 1. Pathway used for the synthesis of compound **7**.

(3.13 mL, 1 eq). The resulting mixture was stirred at 0° for 1 hr and at room temperature for 12 hr. After concentration, the residue was treated with aqueous Na_2CO_3 (10%), and the mixture was extracted with CH_2Cl_2 (3 × 100 mL). The organic fractions were pooled, washed with saturated aqueous NaCl, dried over $MgSO_4$ and concentrated *in vacuo*. The residue was applied to a column packed with silica gel, and the column was eluted (CH_2Cl_2:isopropanol, 95:5). The fractions containing the product with an Rf = 0.66 were pooled and concentrated *in vacuo* to an oil (7 g, 90%): ^{1}H-NMR ($CDCl_3$) δ 7.25 (m, 3H), 6.85 (m, 2H), 4.45 (d, 2H, J = 6 Hz), 4.3 (s, 1H), 3.85 (s, 3H), 3 (m, 2H), 1.2 (m, 12H). Anal. ($C_{16}H_{25}NO_2S_2$) C, H, N.

*2.1.3. N1-(2-Methoxybenzyl)-2-oxoacetamide (**5**)*

To a solution of **4** (5 g, 15 mmol) in water:acetonitrile 20:80 (100 mL) cooled at 0° was added dropwise a solution of *N*-bromosuccinimide (3.2 g, 18 mmol) in acetonitrile (20 mL). The mixture was stirred at 0° for 15 min and poured in a mixture of water:CH_2Cl_2 1:1 (100 mL). The mixture was shacked and washed with CH_2Cl_2 (2 × 100 mL). The organic layers were pooled, dried over $MgSO_4$ and evaporated. Column chromatography through silica gel (ethyl acetate) gave **5** as an oily residue (1.8 g, 63%): ^{1}H-NMR ($CDCl_3$) δ 9.3 (s, 1H), 7.5 (t, 1H, J = 7 Hz), 7.25 (m, 2H), 6.85 (m, 2H), 4.45 (d, 2H, J = 7 Hz), 3.8 (s, 3H).

*2.1.4. 3-Hydroxy-3-phenylpropylamine (**6**)*

To a mixture of $LiAlH_4$ (2 g, 55 mmol) in anhydrous tetrahydrofuran:ether 1:1 (40 mL) at 0° was added dropwise a solution of benzoylacetonitrile (2 g, 13.8 mmol) in tetrahydrofuran:ether 1:1 (25 mL). The mixture was then stirred and heated at reflux for 12 hr. After cooling (0°), water (2.28 mL) was slowly added and the mixture was stirred for 30 min, then aqueous NaOH 15% (2.28 mL) and water (6.8 mL) were successively added. The mixture was filtrated and the filtrate was dried ($MgSO_4$) and evaporated. The residue was distilled ($E_{0.2}$ = 120°) giving rise to **6** as a white solid (1 g, 50%): mp 60°; ^{1}H-NMR ($CDCl_3$) δ 7.37–7.22 (m, 5H), 4.9–4.8 (m, 1H), 3–2.8 (m, 5H), 1.8–1.74 (m, 2H). Anal. ($C_9H_{13}ON$) C, H, N.

*2.1.5. N2-(2-Methoxybenzyl)-6-phenyl-1,3-oxazinane-2-carboxamide (**7**)*

In a round bottomed flask equipped with a Dean–Stark apparatus containing a solution of **5** (0.7 g, 3.6 mmol) in benzene (12 mL) were added pyridinium *p*-toluene sulfonate (15 mg) and **6** (1 g, 6.6 mmol). The mixture was refluxed for 4 hr and evaporated. Column chromatography through silica gel (CH_2Cl_2:isopropanol, 96:4) of the residue gave **7** as a white solid (0.45 mg, 38%): mp 108–111°; ^{1}H-NMR ($CDCl_3$) δ 7.36–7.2 (m, 8H), 6.9–6.8 (m, 2H), 4.77 (s, 1H), 4.69–4.62 (m, 1H), 4.5 (d, 2H, J = 6 Hz), 3.78 (s, 3H), 3.4–3.3 (m, 1H), 3.2–3 (m, 1H), 2 (s, 1H), 1.8–1.6 (m, 2H). Anal. ($C_{19}H_{22}O_3N_2$) C, H, N.

*2.1.6. N2-Benzyl-2-quinolinecarboxamide (**8**) and N2-(2-cyclohexyl)-2-quinolinecarboxamide (**9**)*

Compounds **8** [20–22] and **9** [23] previously described, were classically synthesised through the chloride derivative of 2-quinolinecarboxylic acid.

*2.1.7. Copper(II) complexation of N2-(2-methoxybenzyl)-6-phenyl-1,3-oxazinane-2-carboxamide (**C7**)*

A solution of $Cu(ClO_4)_2{\cdot}6H_2O$ (123 mg in 15 mL of methanol) was added to 109 mg of compound **7** previously dissolved in 15 mL of methanol to give a transparent blue solution. After several days, dark blue and light blue crystals were formed. The dark blue crystals were dissolved in acetonitrile and the solution was placed into a closed area saturated with diethyl ether vapour. Large blue crystals that desegregate in air deposit.

*2.1.8. Copper(II) complexation of N2-benzyl-2-quinolinecarboxamide (**C8**)*

A solution of $Cu(ClO_4)_2{\cdot}6H_2O$ (350 mg in 5 mL H_2O) was added to 262 mg of compound **8** previously dissolved in 20 mL of methanol. Yellow-green crystals were formed which became opaque in air.

*2.1.9. Copper(II) complexation of N2-(2-cyclohexyl)-2-quinolinecarboxamide (**C9**)*

A solution of $Cu(ClO_4)_2{\cdot}6H_2O$ (370 mg in 5 mL of methanol) was added to 202 mg of compound **9** previously dissolved in 20 mL of methanol to form, after a few days, green crystals.

2.2. Biological evaluation

HIV-1 protease was kindly supplied by H.J. Schramm, Max Planck Institut für Biochimie (Martinsried, Germany). It was expressed using the plasmid pET9c-PR, isolated and purified as described by Billich *et al.* [24]. The recombinant protease mutant C67A, C95A was a gift from D.A. Davis (National Institutes of Health, Bethesda, USA). The fluorogenic substrate Dabcyl-γ-Abu-S-Q-N-Y-P-I-V-Q-Edans (Dabcyl, 4-(4-dimethylaminophenylazo)-benzoic acid; Edans, 5-[(2-aminoethyl) amino]naphthalene sulfonic acid; γ-Abu, aminobutyric acid) was purchased from Bachem. The fluorescence-based assays were performed using a LS 50B Perkin Elmer luminescence spectrofluorometer equipped with a thermostated cell holder. The spectral evolution were followed using an Uvikon 941 spectrophotometer.

2.3. Enzyme inhibition

Enzymatic assays were performed either in 100 mM sodium acetate, 100 mM NaCl, 3% Me_2SO (v/v) at pH 5.5, or in 25 mM sodium phosphate, 100 mM NaCl, 3% Me_2SO (v/v) at pH 6.0 or 6.5 and 30°. The inhibitory effect of metal-organic compounds **C1**, **C2**, **C7**, **C8**, **C9** were

compared with that of $CuCl_2$ at pH 5.5 (mutant protease) and pH 6.0 or 6.5 (wild-type protease) in the following conditions: 0.52 μL of a 3 mM solution of substrate (final concentration, 5.2 μM) was added to 8.5 μL of various concentrations of inhibitor or $CuCl_2$ (0.5–4.7 μM) in a final volume of 300 μL. The assays were started with the addition of HIV-1 PR (final concentration, 22.7 nM) or mutant protease (final concentration, 97.8 nM) prediluted in buffer containing 1 mg/mL bovine serum albumin. The change in fluorescence at 490 nm ($\lambda_{exc} = 340$ nm) was monitored over a period of 5 min, 30 s after the addition of enzyme. The dependence of the inhibitory effect of **C1** towards wild-type protease on time was analysed at pH 5.5 and 30° using the progress curve method as previously described [25]. The first derivatives of the progress curve (or velocities v) for the variation with time of the fluorescence at 490 nm ($\lambda_{exc} = 340$ nm) were computer-calculated using Kaleidagraph version 3.0.1 from Abelbeck Software. The parameter π was obtained by fitting the data in the equation: $v = v_0 e^{-\pi t}$. The inactivation constants k_i and K_I were obtained by non-linear regression fitting of the experimental data to the equation $\pi = k_i[I]\ (1-\alpha)/[K_I + [I](1-\alpha)]$, with $\alpha = [S]/K_m + [S]$, $[S]$ is the initial substrate concentration, $[I]$ the inhibitor concentration and K_m the Michaelis constant for the substrate with $K_m = 103$ μM [26]. Enzyme, substrate and inhibitor **C1** concentrations were 7.5 nM, 5.2 μM, 0.55–22 μM, respectively.

2.4. Electron paramagnetic resonance spectroscopy

Electron paramagnetic resonance (EPR) study was performed at room temperature in the X-band region with a Bruker ESP 300 E spectrometer equipped with a TM110 cavity. The samples (compounds **C1**, **C2**, **C7**, **C8**, **C9**, and $Cu(OAc)_2$, 5 mM) were prepared in a 100 mM acetate buffer at pH 5.5 or in methanol and immediately transferred into a quartz flat cell. The experimental settings were as follow: 100 kHz modulation frequency; microwave frequency 9.55 GHz; microwave power 10 mW; sweep width 1000 G; centre field 3120 G; time conversion 81.92 ms; time constant 163.84 ms; receiver gain 2×10^4; and number of scan 4.

2.5. Molecular modelling

All molecular mechanic calculations were performed with the DISCOVER module in the INSIGHT II software (Biosym/Molecular Simulations Inc., San Diego, version 97.0) on MSI Silicon Graphics Indigo 2 workstations. The initial HIV-1 PR structure was the X-ray crystal form of HIV-1 PR solved by Erickson *et al.* [27]. The previously obtained crystal co-ordinates of compound **C1** [9] were used for docking into the active site of HIV-1 PR. Four orientations were considered allowing the pyridyl groups to bind either to the S1/S′1 or S2/S′2 pockets. The resulting complexes formed between the enzyme and compound **C1** (where the crystal apical methanol co-ordinates were substituted by more relevant physiological water molecules) were submitted to a minimisation procedure, using the esff metal adapted forcefield [28]. At the end of the procedure, the energy of interaction between **C1** and PR was computed for the various orientations [29]. In the most favourable orientation, the pyridyl group occupies the S2/S′2 pockets. *Ab initio* calculations on ligands **1**, **2**, **8** and **9** were performed with an optimisation procedure in the framework of

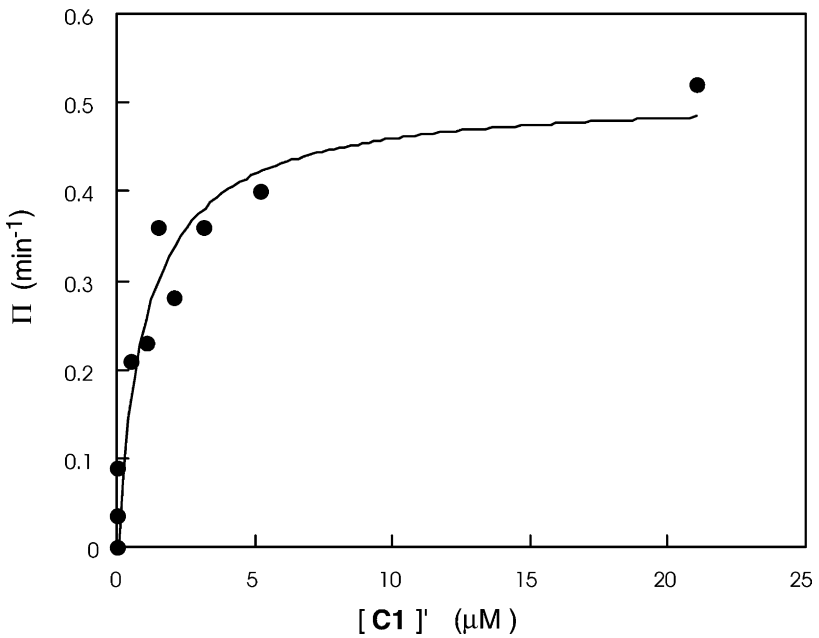

Fig. 4. Inactivation of HIV-1 PR by **C1** at pH 5.5 and 30°. The enzyme (7.5 nM) was incubated in 100 mM sodium acetate, 100 mM NaCl, 3% (v/v) Me_2SO with the fluorogenic substrate Dabcyl-γ-Abu-S-Q-N-Y-P-I-V-Q-Edans (5.2 μM) in the presence of various concentrations of **C1** (0.55–22 μM).

the HF-LCAO-MO-SCF formalism. The 3–21 g basis set was used and all the computations were carried out using the Gaussian 98 program. The molecular electrostatic potentials (MEP) were calculated at the HF/6–31 g* level on the crystal conformation.

3. Results and discussion

3.1. Enzyme inhibition

Ligands **1**, **2**, **7**, **8**, and **9** were synthesised and complexed to copper(II). The resulting complexes were tested for their ability to inhibit HIV-1 PR in a purified enzyme system. The inhibition obtained was compared to the effect of cupric ions alone. In fact, it was previously described that cupric chloride ($CuCl_2$) can also act as an inhibitor of HIV-1 PR by targeting the sulfhydryl group of cysteines instead of acting at the catalytic site of the enzyme [30,31]. It was shown that a mutant protease where cysteine 67 and 95 residues were mutated to alanine was not inhibited by cupric ions [30]. When tested, complex **C1** was found to behave as a time-dependent inhibitor of wild-type HIV-1 PR. The kinetic parameters for the inactivation process were determined using the progress curve method in which the substrate and the inhibitor compete (Fig. 4). At 30° and pH 5.5, the inactivation efficiency index k_i/K_I was equal to 7.730 $M^{-1}\,s^{-1}$, and k_i and K_I to $8.5 \times 10^{-3}\,s^{-1}$ and 1.1 μM, respectively. To discriminate between a putative effect of the decomplexed cupric ion (known to be an inactivator) from the metal-organic complex and the effect of the complex itself (supposed to act as a reversible inhibitor), the inhibitory efficiencies of compound **C1** and $CuCl_2$ were compared in a phosphate buffer using equal concentrations of the two molecules at pH 6.0 and 6.5. The compounds were incubated for 30 s with the wild-type enzyme before determination of the remaining activity. As shown in Fig. 5a, inhibition of HIV-1 PR by **C1** and $CuCl_2$ led to two different sigmoid curves demonstrating that the inhibition due to **C1** was dual: part of the inhibition could be attributed to free Cu^{2+} (released from the complex), the difference between the two curves corresponding to the true effect of the metal-complex. An estimation of the K_i values for the interaction between complex **C1** and HIV-1 PR, and $CuCl_2$ and HIV-1 PR, was obtained by

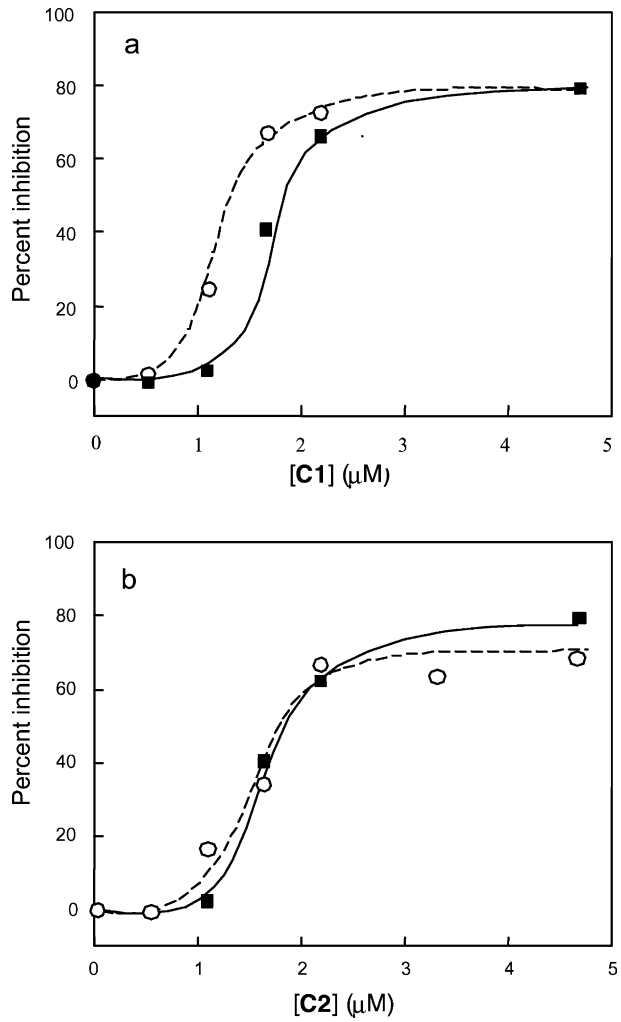

Fig. 5. Inhibition of HIV-PR (22.7 nM) by **C1** (○, a), **C2** (○, b) and $CuCl_2$ (■, a and b) at pH 6.5 and 30°. The enzyme was added in 0.025 M Na phosphate, 0.1 M NaCl, 3% Me_2SO (v/v), containing the fluorogenic substrate Dabcyl-γ-Abu-S-Q-N-Y-P-I-V-Q-Edans (5.2 μM) and different concentrations of **C1** (0–2.2 μM, a), **C2** (0–4.7 μM, b) and $CuCl_2$ (0–4.7 μM, a and b).

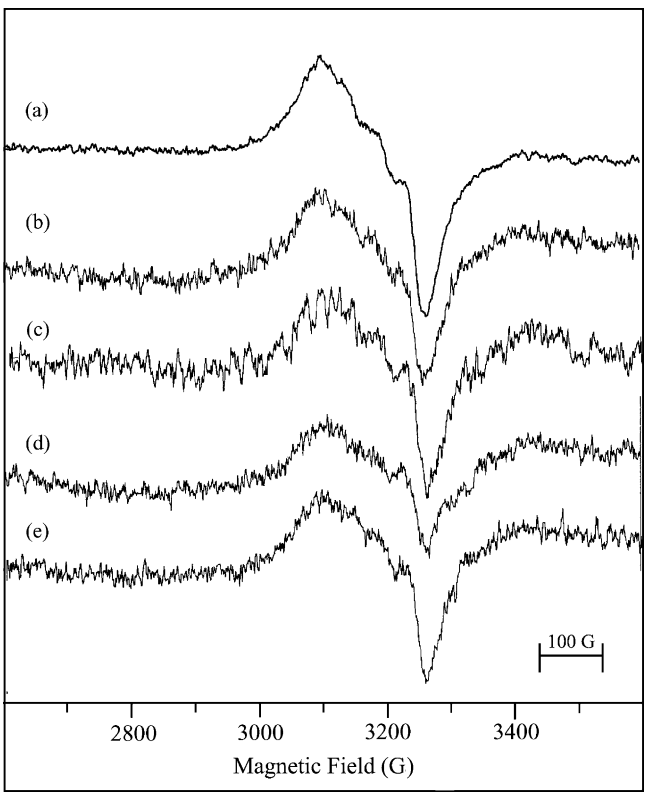

Fig. 6. EPR spectra at room temperature of (curve a) free copper(II), (curve b) **C2**, (curve c) **C7**, (curve d) **C8**, and (curve e) **C9** recorded in the acetate buffer (pH 5.5).

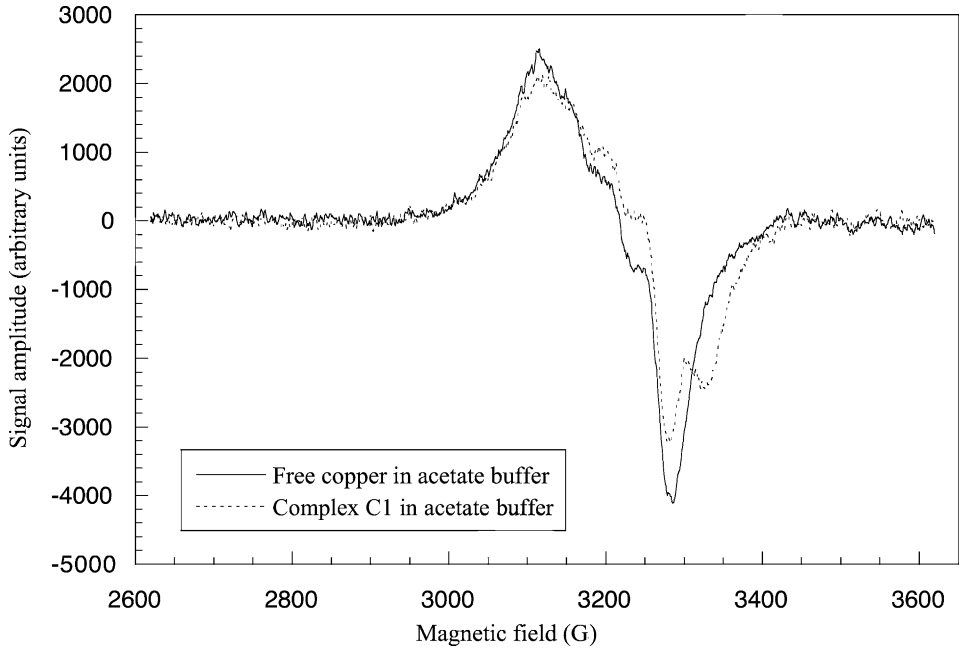

Fig. 7. Comparison of the spectrum of free copper(II) (solid line) and complex **C1** (dashed line) at room temperature. Both spectra were normalised to the same integrated intensity. Concentration of **C1**: 1 mM, acetate buffer (pH 5.5).

plotting $\log(v/v_i)$ as a function of $1 + [I]/K_i$ for a competitive type of inhibition (v and v_i represent the initial rate in the absence and in the presence of the inhibitor, respectively with $S_0 \ll K_m$). A similar inhibitory constant K_i was found for the metal-complex and $CuCl_2$ (~1 μM). The value obtained for $CuCl_2$ confirms the global K_I value determined by the progress curve method for the inactivation process. For compounds **C2** (Fig. 5b), **C7**, **C8**, and **C9**, the inhibition curves were superimposable to that obtained for $CuCl_2$ using the same concentration of reagents and upon 30 s incubation with the enzyme. This confirms that the corresponding complexes are not stable enough in the assay buffer to inhibit the enzyme. In these cases, the inhibitory effect was fully attributed to free cupric ion decomplexed from the metal-compounds. To confirm the observed inhibition of HIV-1 PR, the ability of metal compound **C1** to inhibit a recombinant protease devoid of cysteine residue (C67A, C95A) [18] was examined. We found that the mutant protease was inhibited (>20%) in the presence of 1.7–2 μM of compound **C1** whereas no inhibitory effect was observed

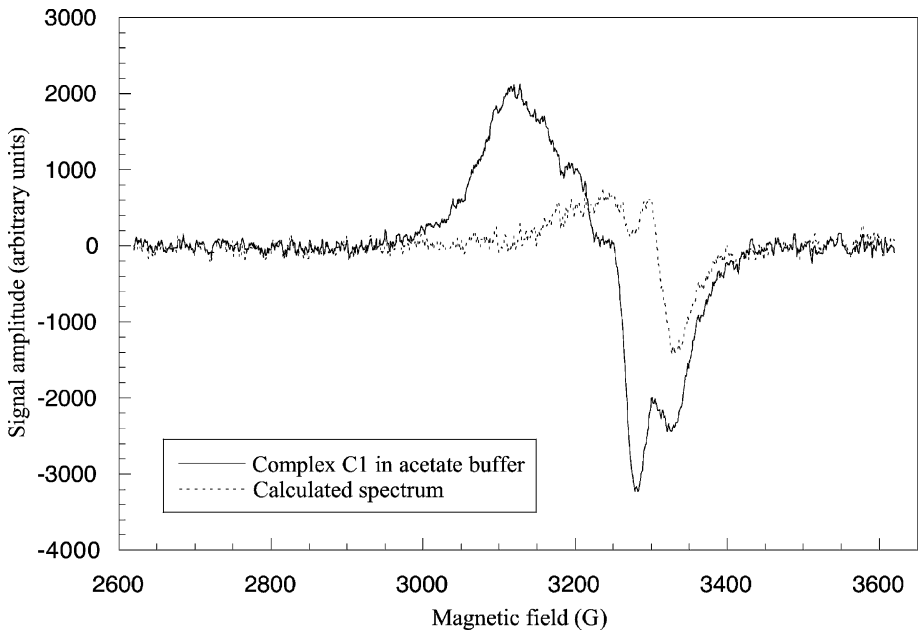

Fig. 8. Comparison of the EPR spectrum of complex **C1** (solid line) in the acetate buffer and calculated EPR spectrum (dashed line). The latter was obtained by subtracting the EPR signal of copper(II) to the EPR spectrum of complex **C1** in the acetate buffer.

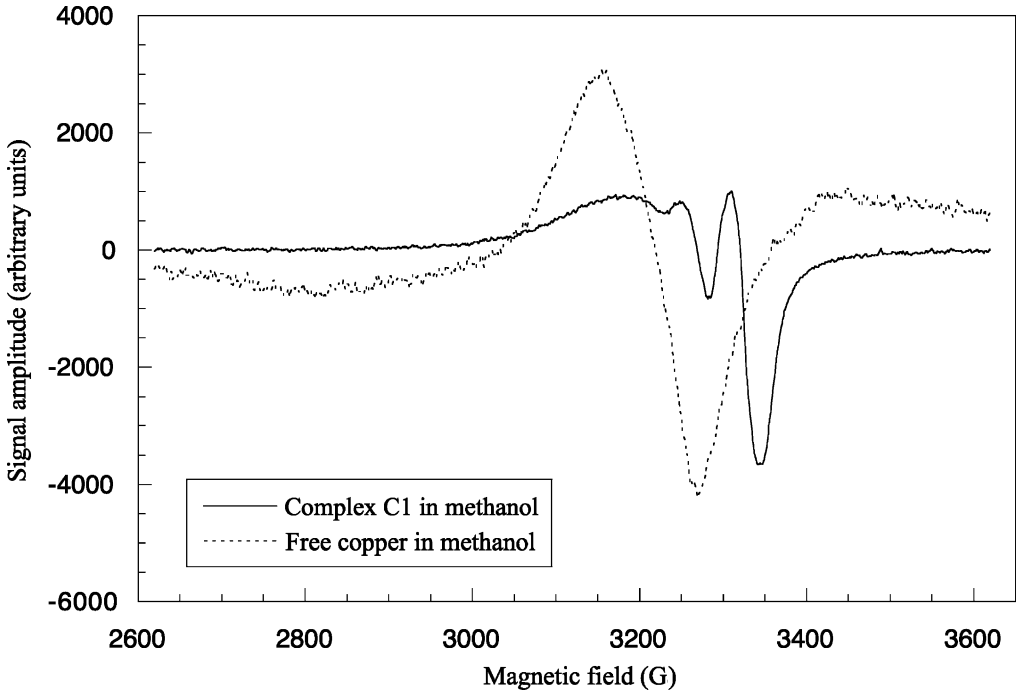

Fig. 9. Comparison of the EPR spectrum of complex **C1** in methanol (solid line) and EPR spectrum of free copper in methanol (dashed line).

using the same concentrations of $CuCl_2$. In contrast, compounds **C2**, **C7**, **C8**, and **C9** failed to inhibit the mutant protease at 0.5–5 μM. These results are in agreement with the work of Karlström and Levine [30] who demonstrated that only copper chelates (and not cupric ions) act as inhibitors of the mutant protease.

3.2. Electron paramagnetic resonance characterisation

An EPR analysis was performed in order to determine whether the studied complexes remained stable in the enzymatic assay buffer (acetate buffer, pH 5.5). The comparison of the spectrum of the free Cu(II) sample with the

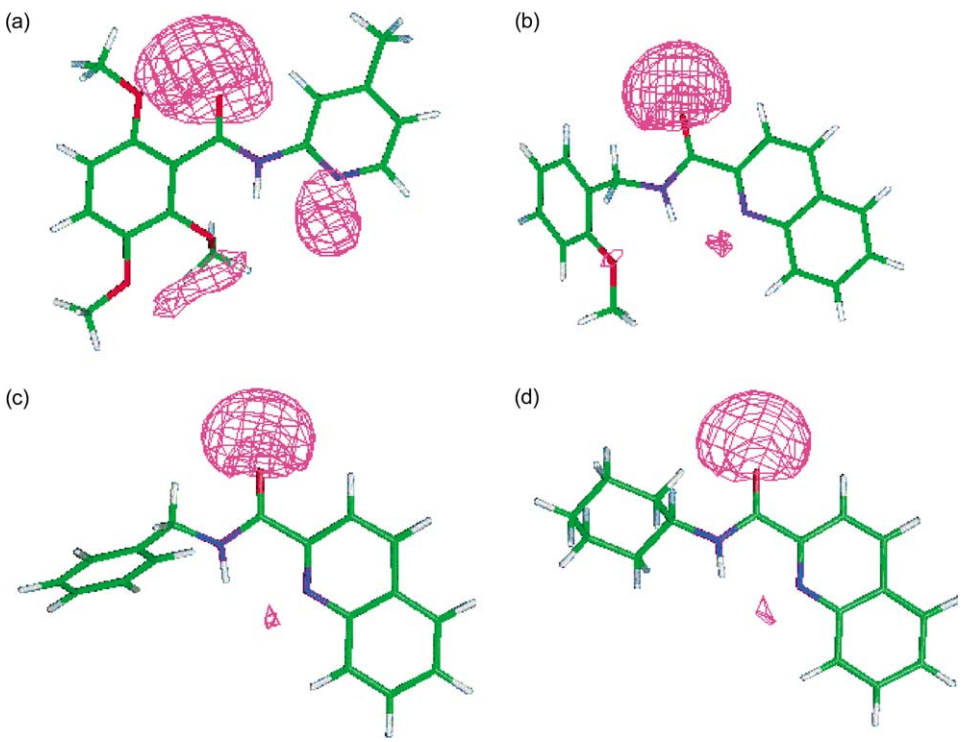

Fig. 10. MEP at −30 kcal/mol calculated for ligands **1**, **2**, **8**, and **9** (HF/6–31 g*). Carbon atoms are depicted in green, nitrogen and oxygen atoms in violet and red respectively and hydrogen atoms are represented in white.

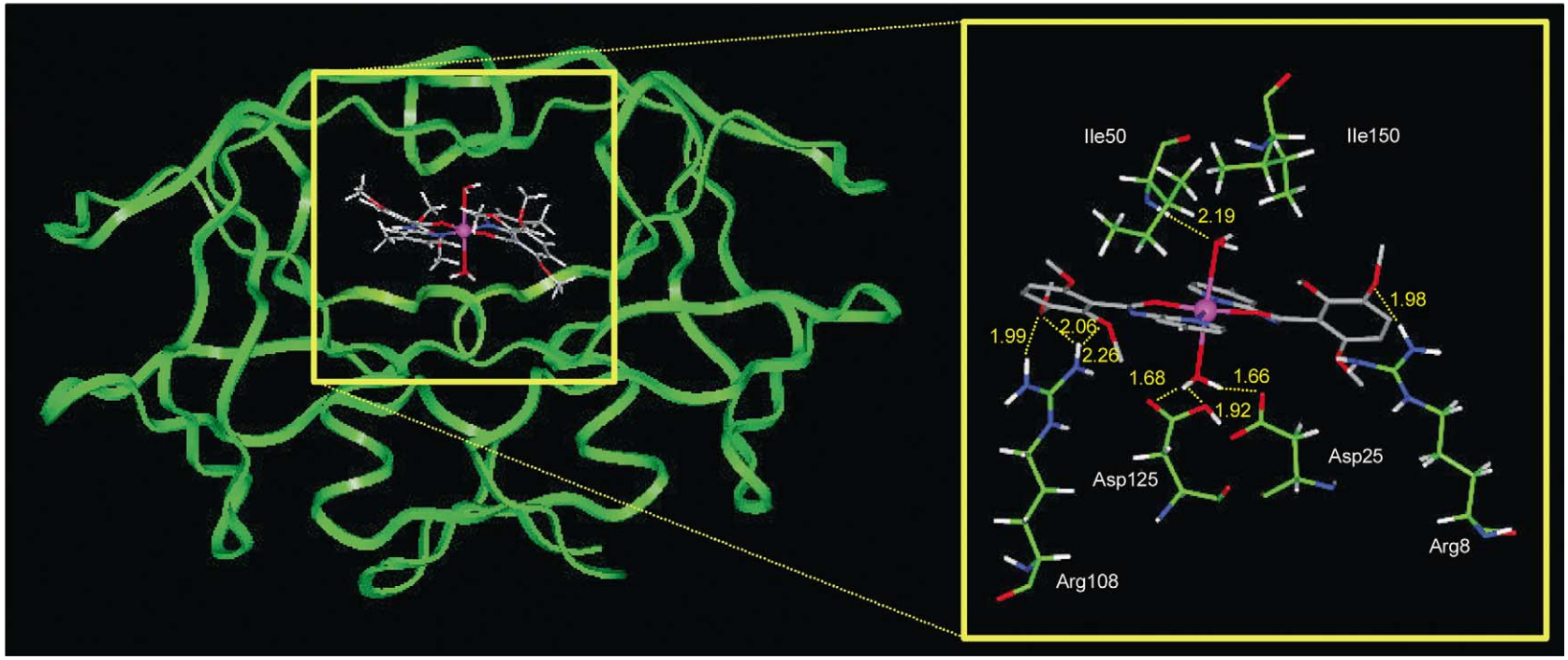

Fig. 11. Interaction between HIV-1 PR and compound **C1** (carbon atoms in gray) as predicted by molecular mechanics simulations and minimisation. For clarity only residues 8, 25, and 50 in both monomers are represented (carbon atoms in green). Nitrogen and oxygen atoms are represented in violet and red, respectively. Hydrogen bonds (Å) are formed between **C1** and residues Asp25, Asp125, Ile50, Arg8, and Arg108.

spectra of complexes **C2**, **C7**, **C8**, and **C9** shows a similar profile characterised by a single broad line centred at around 3300 G (Fig. 6, curves a–e). This first observation seems to indicate that the metal ion was totally released in the medium, thus leading us to assume the lack of stability of the studied complexes in the enzymatic assay buffer. In contrast to the previously studied complexes, the EPR spectrum of **C1**, recorded under the same conditions, exhibits a different shape profile as illustrated in Fig. 7. This difference allows us to assume that a second compound exists in solution in addition to the free copper(II) component. In order to better understand the behaviour of **C1** in the conditions of the enzymatic assay buffer, a comparison was made between the EPR spectrum of **C1** found in the acetate buffer (Fig. 8, solid line) and the calculated spectrum (Fig. 8, dashed line) resulting from the subtraction of the free copper(II) from the total spectrum of **C1** in acetate buffer. The resulting spectrum is in agreement with literature data in which similar Cu(II) complexes exhibit two main lines located between 3000 and 3500 G [32]. To confirm this hypothesis, the EPR spectrum of complex **C1** was recorded in methanol and compared to that of free copper(II) in the same solvent. Indeed, we previously showed that **C1** exists as a complex in MeOH [9]. It appears that the spectrum of **C1** exhibits a more resolved structure in comparison to the spectrum obtained in the acetate buffer. The spectrum of **C1** in MeOH has two main lines located around 3200 and 3350 G (Fig. 9, solid line) vs. the main line for the free copper(II) (Fig. 9, dashed line). This profile is mostly identical to the one obtained for the previously calculated spectrum of **C1** in the acetate buffer (Fig. 8, dashed line). Therefore, one can state that **C1** exists in the enzymatic assay buffer but releases copper(II) in a slow process. Although qualitative, the EPR analysis suggests that compound **1** is the only ligand that remains chelated to copper(II) under the conditions of the enzymatic assay and could be considered as a more stable ligand relative to the other ones studied.

3.3. Molecular modelling

We investigated the reason for the difference in stability between the **C1**, **C2**, **C8**, and **C9** complexes by calculating the MEP on the respective *N*2-pyridine-amide ligands **1**, **2**, **8**, and **9** (Fig. 10). A large attractive area was observed on the pyridyl nitrogen atom of compound **1** involved in the N–Cu bond. In contrast, a much smaller attractive area was present on the corresponding nitrogen atom in compounds **2**, **8**, and **9**. In those compounds, the carbonyl linked at the *ortho* position of the aromatic ring acts as a strong electron attractor, withdrawing electron density from the nitrogen involved in the N–Cu bond. Moreover, the attractive area located on the carbonyl group of ligand **1** is reinforced by the trimethoxyphenyl donor group. The enhanced stability of the N–Cu and O–Cu bonds allows **C1** to exist in the assay buffer. The previously obtained crystal co-ordinates of compound **C1** [9] were used for docking into the active site of HIV-1 PR (Fig. 3b). Molecular modelling studies were performed on the complex formed between HIV-1 PR and **C1** using the metal adapted forcefield esff [28]. The results suggest that **C1** is able to co-ordinate the catalytic water molecule which remains hydrogen bonded to the essential active site residues Asp25 and Asp125. A solvent water molecule is a candidate for the co-ordination of the remaining apical position of the complex and interacts with the flap residue Ile50. In the most favourable orientation, the pyridyl group occupies the S2/S′2 pockets while the trimethoxybenzyl group occupies the larger S1/S′1 subsite (nomenclature of Schechter and Berger [33]). The oxygen atom of the methoxy in the *ortho* and/or *meta* position of the two trimethoxyphenyl groups interacts with the guanidinium group of Arg8 and Arg108 residues (Fig. 11).

4. Conclusion

The interaction pattern derived by molecular modelling is consistent with a competitive inhibition involving two types of interactions: (1) ''Metal-based''—the copper ion present in complex **C1** is properly positioned to chelate the structural catalytic water molecule that initiates the proteolytic reaction. (2) ''Organic-based''—the chelating ligand is involved in several hydrogen bonds and van der Waals contacts with the enzyme. It contributes to interaction specificity and to the global stabilisation of the inhibitor within the enzyme binding cleft. Ongoing crystallographic experiments will help confirming the dual aspect of the interaction of metal-organic complexes with HIV-1 PR. Optimising the interaction of complex setcez with the hydrophobic subsites of HIV-1 PR active site led to the design of a novel co-ordination compound **C1**, with a binding affinity increased by a factor 10^3. Based on the molecular modelling of compound **C1** into the active site of HIV-1 PR, ligands that are better structural and chemical complements of the HIV-1 PR binding site are being designed. Complex **C1** which possesses trimethoxybenzyl groups to interact into the S1/S′1 subsites is rather large for HIV-1 PR active site. However, those methoxy groups are partially responsible for the higher stability of **C1** in the assay buffer, compared to the other *N*2-pyridine-amide ligands studied. Therefore, when designing the new ligands, we have to keep in mind that the stability of the final complex in the assay buffer is crucial to the true inhibition observed. One way to ensure stability is to consider more chelating polydentate ligands. The proper understanding of the unique structural paradigm of metal-organic complexes should eventually lead to the development of potent and highly selective inhibitors of HIV-1 PR. The expertise and comprehension gained in the framework of HIV-1 PR will prove useful for the specific inhibition of enzymes containing sites likely to bind a metal ion [15]. While metal cations are not likely to be useful agents,

metal chelates such as **C1** should be considered as promising lead compounds for the development of targeted drugs.

Acknowledgments

The authors wish to thank H.J. Schramm (Max Planck Institut für Biochemie, Martinsried, Germany), D.A. Davis (National Institutes of Health, Bethesda, USA) for providing us with the wild-type protease and the recombinant protease mutant C67A, C95A, respectively and X. Damoiseau for helpful discussions. This work was supported by BIOMED 2 Network (BMH4-CT96-0823). F. Lebon and M. Ledecq thank the National Belgian Foundation for Scientific Research (FNRS) and the Industry and Agriculture Research Foundation (FRIA) for financial support as well as IBM-Belgium and the Facultés Universitaires Notre-Dame de la Paix (FUNDP) for the use of the Namur Scientific Computing Facility. Z. Benatallah thanks "Ensemble contre le Sida", SIDACTION for financial support.

References

[1] West ML, Fairlie D. Targeting HIV-1 protease: a test of drug-design methodologies. TiPS 1995;16:67–75.
[2] Kempf DJ, Sham HL. HIV protease inhibitors. Curr Pharm Des 1996;2:225–46.
[3] Deeks SG, Smith M, Holodniy M, Kahn O. HIV-1 protease inhibitors. A review for clinicians. J Am Med Assoc 1997;277:145–53.
[4] Lebon F, Ledecq M. Approaches to the design of effective HIV-1 protease inhibitors. Curr Med Chem 2000;7:455–77.
[5] Schramm HJ, de Rosny E, Reboud-Ravaux M, Büttner J, Dick A, Schramm W. Lipopeptides as dimerisation inhibitors. Biol Chem 1999;380:593–6.
[6] Bouras A, Boggetto N, Benatalah Z, de Rosny E, Sicsic S, Reboud-Ravaux M. Design, synthesis and evaluation of conformationaly constrained tongs, new inhibitors of HIV-1 protease dimerisation. J Med Chem 1999;42:957–62.
[7] Flexner C. HIV-protease inhibitors. New Engl J Med 1998;338:1281–92.
[8] Molla A, Granneman GR, Sun E, Kempf DJ. Recent developments in HIV protease inhibitor therapy. Antivir Res 1998;39:1–23.
[9] Lebon F, Ledecq M, Benatallah Z, Sicsic S, Lapouyade R, Kahn O, Garçon A, Reboud-Ravaux M, Durant F. Synthesis and structural analysis of copper(II) pyridineamide complexes as HIV-1 protease inhibitors. J Chem Soc, Perkin Trans 2 1999;4:795–800.
[10] Lebon F, de Rosny E, Reboud-Ravaux M, Durant F. De novo drug design of a new copper chelate molecule acting as HIV-1 protease inhibitor. Eur J Med Chem 1998;33:733–7.
[11] Sadler PJ, Inorganic chemistry and drug design. In: Advances in inorganic chemistry, vol. 36. New York: Academic Press, 1991. p. 1–49.
[12] Louie AY, Meade TJ. Metal complexes as enzyme inhibitors. Chem Rev 1999;99:2711–34.
[13] Lippard SJ. In: Bertini I, Gray HB, Lippard SJ, Valentine JS, editors. Bioinorganic chemistry. Mill Valley, CA: University Science, 1994. p. 505–83.
[14] Berners-Price SJ, Sadler PJ. Co-ordination chemistry of metallo-drugs: insights into biological speciation from NMR spectroscopy. Coord Chem Rev 1996;151:1–40.
[15] Katz BA, Clark JM, Finer-Moore JS, Jenkins TE, Johnson CR, Ross MJ, Luong C, Moore WR, Stroud RM. Design of potent selective zinc-mediated serine protease inhibitors. Nature 1998;391:608–12.
[16] Janc JW, Clark JM, Warne RL, Elrod KC, Katz BA, Moore WR. A novel approach to serine protease inhibition: kinetic characterisation of inhibitors whose potencies and selectivities are dramatically enhanced by zinc(II). Biochemistry 2000;39:4792–800.
[17] DeCamp DL, Babe LM, Salto R, Lucich JL, Koo M-S, Kahl SB, Craik CS. Specific inhibition of HIV-1 protease by boronated porphyrins. J Med Chem 1992;35:3426–8.
[18] Davis DA, Branca AA, Pallenberg AJ, Marschner TM, Patt LM, Chatlynne LG, Humphrey RW, Yarchoan R, Levine RL. Inhibition of the human immunodeficiency virus-1 protease and human immunodeficiency virus-1 replication by bathocuproine disulfonic acid Cu^{1+}. Arch Biochem Biophys 1995;322:127–34.
[19] Qasmi D, de Rosny E, René L, Badet B, Vergely I, Boggetto N, Reboud-Ravaux M. Synthesis of *N*-glyoxylyl peptides and their in vitro evaluation as HIV-1 protease inhibitors. Bioorg Med Chem 1997;5:707–14.
[20] Benincori T, Brenna E, Sanniedo F. Studies on Wallach's imidazole synthesis. J Chem Soc, Perkin Trans 1 1993;675–80.
[21] Gracheva IN, Ioffina DI, Tochilkin AI, Gorkin VZ. Monoamine oxidase based on 2-, 4-, and 8-substituted quinolines. Pharm Chem J 1991:160–5 [English translation].
[22] Piechaczek B-D. Studies on monoamine oxidase inhibitors. VII. Derivatives of quinolinecarboxylic acids. Acta Pol Pharm 1966;9–14.
[23] Coppa F, Fontana F, Lazzarini E, Minisci F. A facile convenient and selective homolytic carbamoylation of heteroaromatic bases. Heterocycles 1993;2687–96.
[24] Billich A, Hammerschmid F, Winkler G. Purification, assay and kinetic features of HIV-1 protease. Biol Chem Hoppe-Seyler 1990;371:265–72.
[25] Doucet C, Pochet L, Thierry N, Pirotte B, Delarge J, Reboud-Ravaux M. 6-Substituted 2-oxo-2H-1-benzopyran-3-carboxylic acid as a core structure for specific inhibitors of human leukocyte elastase. J Med Chem 1999;42(20):4161–71.
[26] Matayoshi ED, Wang GT, Krafft GA, Erickson J. Novel fluorogenic substrates for assaying retroviral proteases by resonance energy transfer. Science 1990;247:954–8.
[27] Erickson J, Neidhart DJ, VanDrie J, Kempf DJ, Wang XC, Norbeck DW, Plattner JJ, Rittenhouse JW, Turon M, Wideburg N, Kohlbrenner WE, Simmer R, Helfrich R, Paul DA, Knigge M. Design, activity, and 2.8 Å crystal structure of a C2 symmetric inhibitor complexed to HIV-1 protease. Science 1990;249:527–33.
[28] Biosym/MSI, Discover user guide, vol. 1. San Diego, 1995.
[29] Holloway MK, Wai JM, Halgren TA, Fitzgerald PMD, Vacca JP, Dorsey BD, Levin RB, Thompson WJ, Chen LJ, Desolms SJ, Gaffin N, Ghosh AK, Giuliani EA, Graham SL, Guare JP, Hungate RW, Lyle TA, Sanders WM, Tucker TJ, Wiggins M, Wiscount CM, Woltersdorf OW, Young SD, Darke PL, Zugay JA. A priori prediction of activity for HIV-1 protease inhibitors employing energy minimisation in the active site. J Med Chem 1995;38:305–17.
[30] Karlström ARK, Levine RL. Copper inhibits the protease from human immunodeficiency virus 1 by both cysteine-dependant and cysteine-independent mechanisms. Proc Natl Acad Sci USA 1991;88:5552–6.
[31] Karlström ARK, Shames BD, Levine RL. Reactivity of cysteine residues in the protease from human immunodeficiency virus: identification of a surface-exposed region which affects enzyme function. Arch Biochem Biophys 1993;304:163–9.
[32] Nagane R, Koshigoe T, Chikira M, Long EC. The DNA-bound orientation of Cu(II)-Xaa-Gly-His metallopeptides. J Inorg Biochem 2001;83:17–23.
[33] Schechter I, Berger A. On the size of the active site in proteases I. Papain Biochem Biophys Res Commun 1967;27:157–62.